sustainability

MDPI

Article

A Carbon-Cloth Anode Electroplated with Iron Nanostructure for Microbial Fuel Cell Operated with Real Wastewater

Enas Taha Sayed [1,2,*], Hussain Alawadhi [1,3], Khaled Elsaid [4,*], A. G. Olabi [1,5,6], Maryam Adel Almakrani [5], Shaikha Tamim Bin Tamim [5], Ghada H. M. Alafranji [5] and Mohammad Ali Abdelkareem [1,2,5,*]

1 Center for Advanced Materials Research, University of Sharjah, Sharjah 27272, UAE; halawadhi@sharjah.ac.ae (H.A.); aolabi@sharjah.ac.ae (A.G.O.)
2 Chemical Engineering Department, Faculty of Engineering, Minia University, Al Minya 61111, Egypt
3 Department of Applied Physics and Astronomy, University of Sharjah, PO Box, Sharjah 27272, UAE
4 Chemical Engineering Program, Texas A&M University, College Station, TX 77843-3122, USA
5 Department of Sustainable and Renewable Energy Engineering, University of Sharjah, Sharjah 27272, UAE; U15105781@sharjah.ac.ae (M.A.A.); U15100502@sharjah.ac.ae (S.T.B.T.); U15105468@sharjah.ac.ae (G.H.M.A.)
6 Mechanical Engineering and Design, School of Engineering and Applied Science, Aston University, Aston Triangle, Birmingham B4 7DA, UK
* Correspondence: e.kasem@mu.edu.eg (E.T.S.); khaled.j.elsaid@gmail.com (K.E.); mabdulkareem@sharjah.ac.ae (M.A.A.)

Received: 22 June 2020; Accepted: 5 August 2020; Published: 13 August 2020

Abstract: Microbial fuel cell (MFC) is an emerging method for extracting energy from wastewater. The power generated from such systems is low due to the sluggish electron transfer from the inside of the biocatalyst to the anode surface. One strategy for enhancing the electron transfer rate is anode modification. In this study, iron nanostructure was synthesized on a carbon cloth (CC) via a simple electroplating technique, and later investigated as a bio-anode in an MFC operated with real wastewater. The performance of an MFC with a nano-layer of iron was compared to that using bare CC. The results demonstrated that the open-circuit voltage increased from 600 mV in the case of bare CC to 800 mV in the case of the iron modified CC, showing a 33% increase in OCV. This increase in OCV can be credited to the decrease in the anode potential from 0.16 V vs. Ag/AgCl in the case of bare CC, to −0.01 V vs. Ag/AgCl in the case of the modified CC. The power output in the case of the modified electrode was 80 mW/m^2—two times that of the MFC using the bare CC. Furthermore, the steady-state current in the case of the iron modified carbon cloth was two times that of the bare CC electrode. The improved performance was correlated to the enhanced electron transfer between the microorganisms and the iron-plated surface, along with the increase of the anode surface- as confirmed from the electrochemical impedance spectroscopy and the surface morphology, respectively.

Keywords: microbial fuel cell; electroplating; electron transfer; iron nanostructure; nanosheet structure; wastewater treatment

1. Introduction

Given the current energy and water challenges facing the world today, new technology should be developed with the aim of facing these problems. Current energy relies on fossil fuels, which not only are limited in resources, but also result in high quantities of pollution and health risks [1–3]. The environmental impact of fossil fuels can be minimized through increasing the efficiency of current technologies [4,5] and/or relying on renewable energy sources [6], such as biomass energy [7–9],

wind energy [10,11], solar thermal energy [12,13], solar PV [14–16], ocean energy [17], and geothermal energy [9]. Fuel cells are emerging energy conversion devices that are silent, have a high theoretical efficiency [18–20], and exhibited high performance when installed in several applications [21,22]. Microbial fuel cells (MFCs) are one of the most promising types of fuel cells, used for simultaneous wastewater treatment and energy harvesting [23–25]. Due to this, this technique is considered as an environmentally friendly technology [26,27]. In the anode side of an MFC, the microorganism metabolite and organic materials contained in the wastewater (or other waste) produce electrons and protons [28,29]. The electrons transfer to the cathode side via an external circuit, where the protons transfer via the electrolyte. At the cathode, electrons and protons combined with oxygen from the air—or any other oxidizing agent—result in the production of water. The structure of the MFC has been modified by different researchers to be used in other promising applications [30,31], such as hydrogen production in microbial electrolysis cells, water desalination in microbial desalination cells, and chemical production in microbial synthesis cells, as summarized by Mohan et al. [32]. Significant efforts have also been made for the scaling up of MFC's, whether through connecting several cells in a series and/or parallel. The progress made in this field and the challenges still facing it are summarized thoroughly by Abbassi et al. [33] and Abdallah et al. [34].

The power output of an MFC is still far from that of a chemical fuel cell [35,36]. The main step in this type of fuel cell is the transfer of the produced electrons from the inside of the microorganism to the anode surface [37]. There are two main mechanisms for electron transfer, direct and indirect. Direct transfer is mainly by the outer membrane cytochrome or trans membrane proteins of the microorganism. This means the microorganism should be in direct contact with the anode surface [23]. The indirect transfer occurs via an endogenous or exogenous mediator to transfer electrons to the anode surface [38,39]. The properties of the bio-anode play a critical part in the performance of MFCs [23,40]. Carbon and carbon-based materials are commonly used as electrodes for MFC as they are cheap, biocompatible, have a good electrical conductivity, and are available in different morphologies, such as carbon paper (CC), carbon cloth, carbon felt, and carbon brush [41–44]. The different parameters affecting the MFC performance include everything from the membrane, electrode type and structure, biocatalyst, cell design, pH, and concentration of the anode [45–48]. In addition, the anode configuration and structure play an important role in cell performance. For instance, the horizontal arrangement of the anode brush with the shortest distance to the cathode demonstrated a 20% increase in the power density, due to the decrease in the overall cell resistance [49]. The usage of a high anode current collector exhibited a 33% increase in the maximum power output, compared to that obtained using a smaller surface area Ti wire anode current collector [50].

Many studies were performed to attempt to enhance MFC performance through anode modification [51]. Modifying the carbon electrode with cobalt, gold, and nickel was investigated as bio-anodes in the MFC [37,52–55]. The performance of the MFC was mainly affected by the type of metal [56]. Cobalt and nickel improved the performance of the MFC, as they are considered essential metals. This means they enhanced both biofilm formation and the rate of electron transfer [37,57]. The nano-gold structures drastically decreased the performance of the yeast-based MFC, as the gold nanostructure poisoned the yeast cell [38]. Iron oxide nanoparticles are another type of transition metal nanoparticles that are cheap, available, biocompatible, and already investigated in different biomedical applications [58–60]. The application of iron oxide nanoparticles prepared by a chemical route followed by depositing the nanoparticles on the surface of a graphite electrode, resulted in the increased performance of the MFC, due to the improvement of the electron transfer between the nanoparticles and the microorganisms [61]. However, despite the preparation method being complicated, the stability and the available surface area are also questionable points.

In this study, a thin layer of nanostructured iron was synthesized on a carbon cloth CC via a simple electroplating technique. This electrode was then used as an anode for MFC, operated with real wastewater without any modifications or additives. The performance of this MFC was compared to

that using plain CC. The results were discussed based on the effect of the plated metal on both the surface area and the electron transfer between the anode and the microorganisms.

2. Material and Methods

2.1. Anode Synthesis

The carbon cloth CC (ElectroChem, Inc.) was dipped in acetone for 10 min, then in deionized water for another 10 min. It was then dried and used as the cathode in the electroplating cell, where the graphite rod was used as the anode. The two electrodes were immersed in 0.16 M of iron chloride (Sigma-Aldrich) and were connected via power supply. The distance between the two electrodes was kept at 1 cm. The electrodes were electroplated at 5 V for 2 min. The iron modified carbon cloth (Fe-CC) was washed several times with distilled water and dried at 50 °C overnight. It was later used as an anode in the MFC.

2.2. Construction of the Microbial Fuel Cell

An air-cathode MFC was constructed with an 84 mL volume for the anode chamber as shown in Figure 1. Nafion 117 (ElectroChem, Inc.) was used as an electrolyte membrane. A ready-made Pt/C on CC of loading of 0.5 mg (fuelcellstore.com) used as the cathode (6 cm^2). The Fe-CC or bare CC of 6 cm^2 was used as the anode. Wastewater from the water treatment plant at Sharjah, U.A.E was used as both a substrate and a microorganism source. The initial COD was in average of 700 ppm. Two MFCs with Fe-CC and bare CC anodes were constructed and operated in parallel under the same operating conditions. Where the anode chamber of the two cells was filled with wastewater, and the two cells were operated at 25 °C in a batch mode.

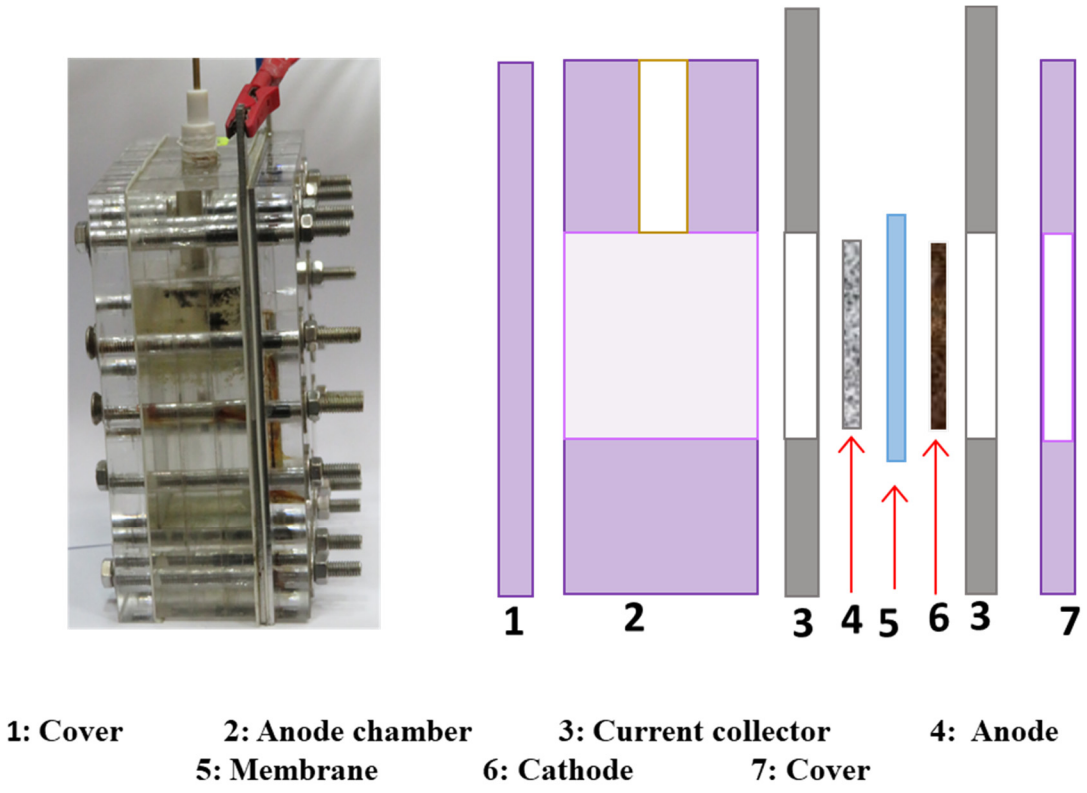

Figure 1. Schematic diagram showing the structure of the microbial fuel cell.

2.3. Electrochemical Measurements

The MFCs were connected with a GL240 multi-channel midi-logger to record the anode potential vs. Ag/AgCl and the open-circuit voltage (OCV). The cell was operated under open circuit conditions until it reached steady state conditions, meaning a constant cell voltage and anode potential. After steady state was achieved, the MFCs were operated under closed-circuit conditions. Linear sweep voltammetry was carried out at 1 mV/s from the open-circuit voltage to zero voltage to obtain the current voltage and current power curves. Then current discharge at 0.2 V was performed for 120 min to investigate the steady-state current generation. The electrochemical impedance spectroscopy (EIS) was conducted for the whole cell at 0.2 V from 100 kHz to 100 mHz.

All the cell measurements under closed-circuit conditions, i.e., linear sweep voltammetry (from open-circuit voltage to zero voltage), current discharge at 0.2 V, and EIS measurements for the whole cell at 0.2 V, were carried out using Potentiostat (Biologic VSP-200).

2.4. Anode Characterization

The surface morphology and the elemental composition of the carbon cloth before and after modification with iron were examined using a scanning electron microscope, SEM (Tescan VEGA XMU) integrated with Energy Dispersive X-Ray (EDX) for elemental analysis.

3. Results and Discussions

3.1. Surface Morphology and Elemental Composition of the Iron Modified Carbon Cloth

Figure 2 shows the surface morphology and elemental analysis of the carbon cloth before and after the deposition of the iron. It is clear from the figure, that the bare carbon cloth is composed of smooth fibers of around 7µm diameter (Figure 2a), that are 100% carbon (Figure 2b). After iron deposition, the surface becomes rough with a Nano sheet structure, as can be seen in (Figure 2c), where the inset shows the high magnification. The surface is composed of iron oxide, as seen in the EDX analysis shown in (Figure 2d).

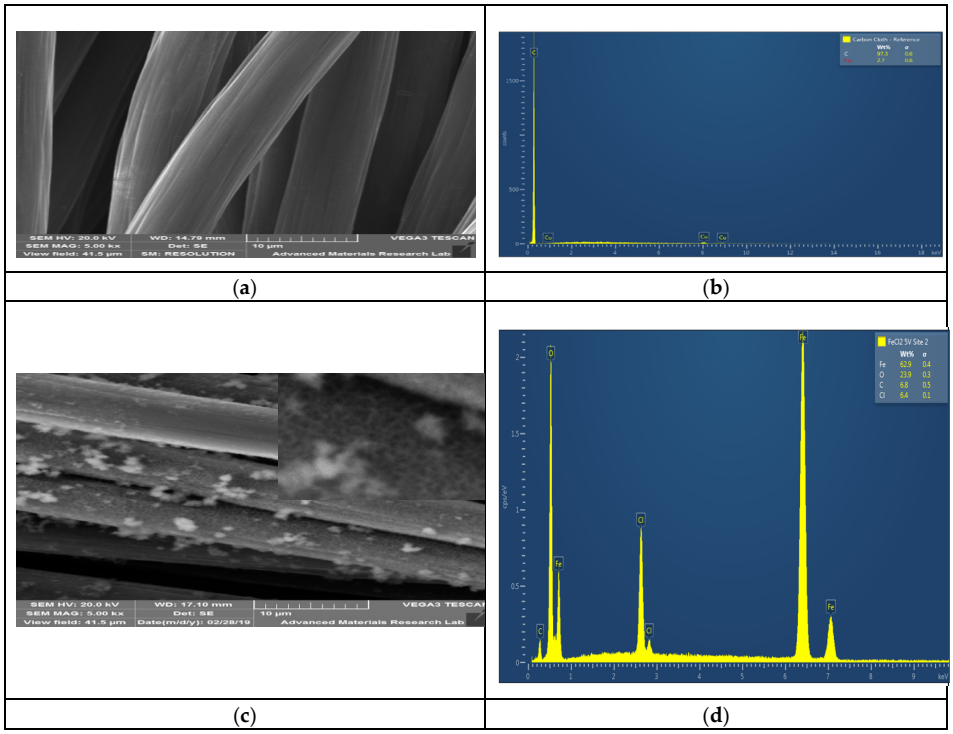

Figure 2. (**a**,**b**) SEM images and EDX elemental analysis of bare carbon cloth and (**c**,**d**) SEM images and EDX elemental analysis of iron modified carbon cloth.

3.2. Microbial Fuel Cells (MFC) Under Open-Circuit Conditions

After the injection of the anolyte solution in the anode chamber, the anode potential vs. Ag/AgCl and open-circuit voltage (OCV) were recorded and shown in Figure 3. As seen in Figure 3a, the anode potential in the case of the cell using the bare CC decreased from 0.22 V vs. Ag/AgCl to reach a minimum value of 0.16 V vs. Ag/AgCl within 30 h. Following that, it was nearly constant. In the case of using Fe-CC on the other hand, the anode potential decreased from an initial value of 0.18 V to reach a minimum value of −0.01 V vs. Ag/AgCl within 40 h. Following that, it was also nearly constant. The decrease of the anode potential in the two cells resulted in the increase in the open-circuit voltage of the two cells, as can be seen in Figure 3b [48]. The steady values of the OCV were 0.79 and 0.62 V, for MFC using Fe-CC and CC, respectively. The higher activity of the Fe-CC compared to the bare CC anode can be credited to the role of the Fe nano-layer in improving the electron transfer between microorganisms. The anode surface can also be credited, due to the role of the iron had improving the electrical conductivity of the CC, as being confirmed later using EIS. Furthermore, the high roughness and the Nano sheet structure of the Fe-CC (Figure 2c) resulted in a higher surface area available for the growth and electron transfer between the microorganisms and the anode surface.

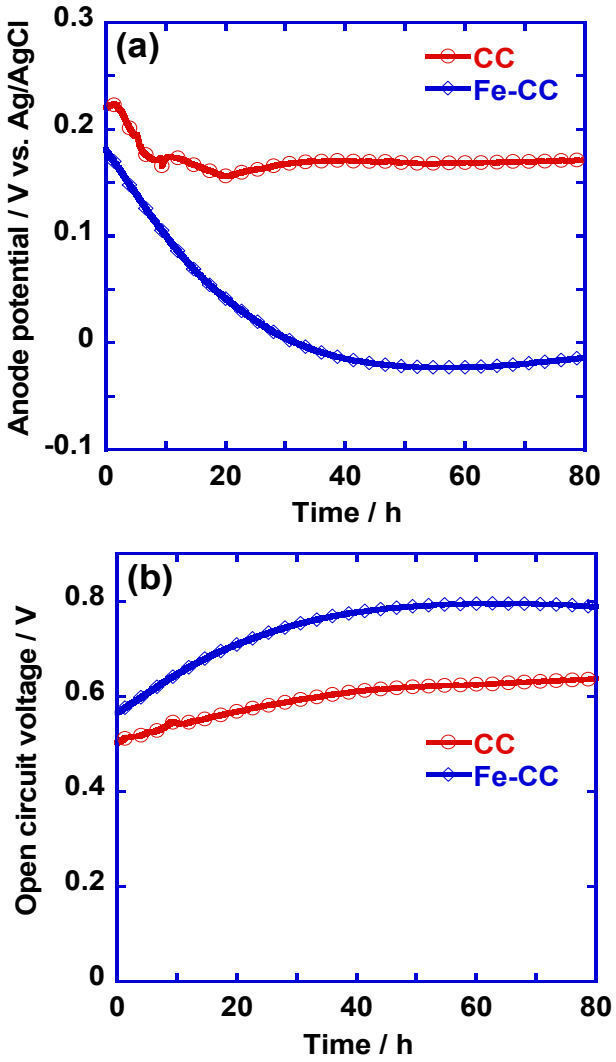

Figure 3. Variation of the anode potential vs. Ag/AgCl with time (**a**) and OCV with time (**b**) of MFC using CC or Fe-CC electrodes.

3.3. Cell Operation Under the Closed-Circuit Condition

Figure 4 shows the performance of two MFCs under closed-circuit conditions. Figure 4a shows the i-V and i-P curves for the two MFCs using the CC and Fe-CC. Modifying the CC with the Fe nanostructure enhanced both the maximum power and current densities of the MFC, as they increased from 40 mW/m^2 and 275 mA/m^2 in the case of CC to 80 mW/m^2 and 890 mA/m^2 in the case of Fe-CC, respectively. This essentially reflects a two-time increase in the power output, and more than a three-time increase in current density. However, the linear sweep voltammetry measurements, i.e., i-V measurements, describe only instantaneous electrode behavior, that could significantly change under long-term operation. Due to this, the cell was operated for around 120 min under a fixed cell voltage of 0.2 V, as shown in Figure 4b. It is clear from the figure, that the cell using the modified electrode, i.e., Fe-CC, demonstrated a significantly higher steady current density, i.e., current after two hours of cell operation, of 134 mA/m^2, is almost two times that obtained in the case of the bare CC of 71 mA/m^2. In both cases, the initial current density rapidly decreases, which could be related to the depletion of the excess electrons, accumulated during the OCV and before the current discharge. However, the slight decrease in the current after this with cell operation (after 10 min of current discharge) especially in the case of the Fe-CC can be attributed to the depletion of the organic materials in the wastewater [23].

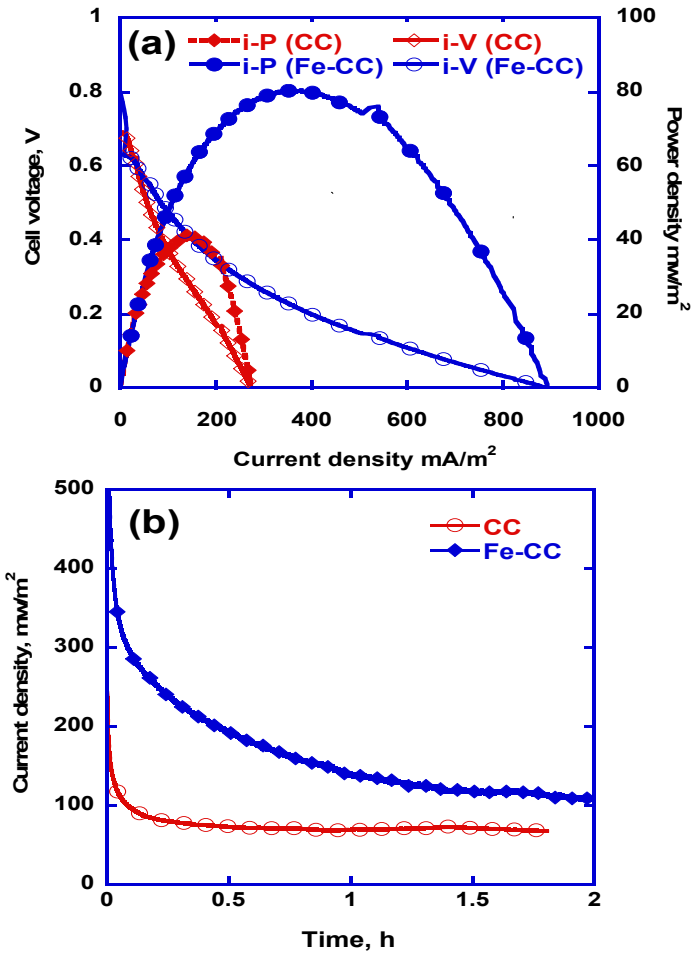

Figure 4. Polarization curves (**a**), current-time discharge at 0.2 V (**b**) of MFCs with CC and Fe-CC.

The enhanced cell performance in terms of the higher power output and higher current density can be attributed to the role of the iron in improving the electrical conductivity of the CC, that increases the electron transfer rate between the microorganisms and the anode, as confirmed from the EIS

measurements shown in Figure 5. As can be seen in the figure, the ohmic resistance of the cell with the Fe-CC electrode is around 2.5 Ohms. This equates to one-third of the ohmic resistance in the case of the bare CC electrode.

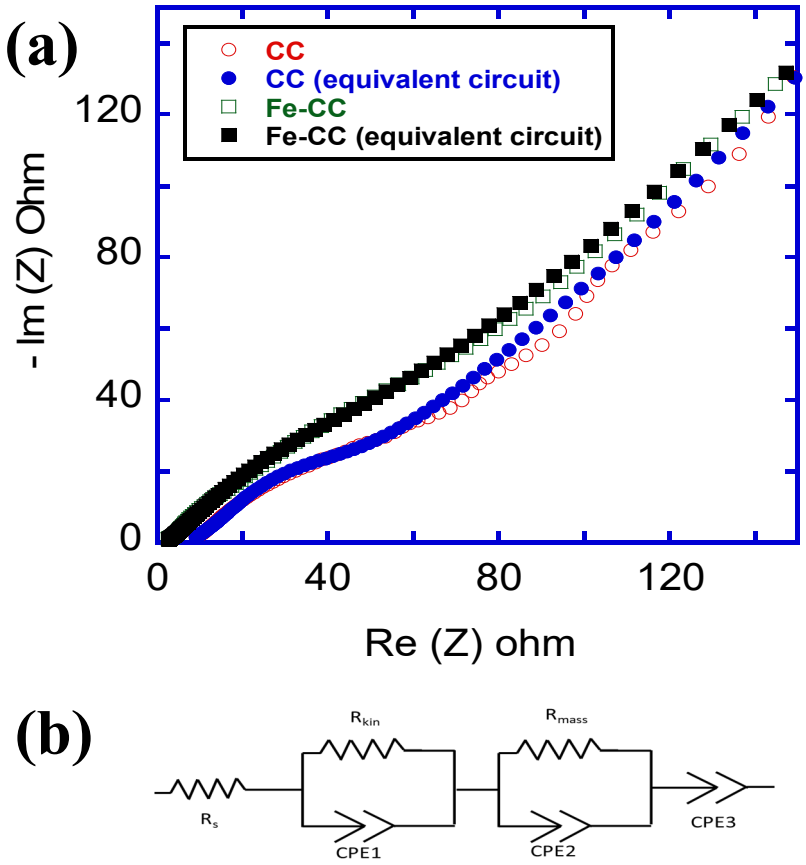

Figure 5. (**a**) Electrochemical impedance spectroscopy (EIS) of MFC with CC or Fe-CC conducted at 0.2 V from 100 kHz to 100 mHz, and (**b**) the equivalent circuit.

Such low resistivity would result in a drastic improvement in the electron transfer from the microorganisms to the anode surface, meaning a higher power output is obtained. Additionally, looking at the linear relationship between the current and voltage in i-V curves for the two cells (Figure 4a), it is clear that the ohmic resistance in the case of the modified electrode is much lower than that in case of the bare CC electrode. Moreover, the high roughness of the modified anode with a nanosheet structure would increase the available surface area of the modified anode, as shown in Figure 2c.

The equivalent circuits in the case of the plain CC and the modified one (Fe-CC) were represented in Figure 5b. As can be seen in the Figure 5b, the circuit is composed of ohmic resistance (Rs) as can be seen at the intersection with the *X*-axis at high frequency, and the slight semi circuit that appears at medium frequency is modeled by the double layer capacitance (CPE1) in parallel to charge transfer resistance (R_{kin}), while at low frequencies, it is modeled by another double layer capacitance (CPE2) that is in parallel to mass transfer resistance (R_{mass}) and both are in series with other double layer capacitance (CPE3) [62].

The values of the different resistances are shown in Table 1:

Table 1. The values of the different resistances of the two cells.

Anode	R_s	R_{kin}	R_{mass}
CC	7.516	60.62	10.52
CC-Fe	1.846	9.27	4.6

It is clear from the table that modifying the carbon cloth with the Fe resulted in significantly decreasing the ohmic resistance from 7.516 to 1.846 ohm, while the charge transfer resistance (R_{kin}) is decreased from 60.62 ohm to 9.27 ohm. Such results confirm the role of the Fe in improving the charge transfer between the microorganisms and the anode surface.

4. Conclusions

The electroplating technique was used for modifying the carbon cloth with a thin layer of an iron nanostructure. The synthesized iron coated carbon cloth Fe-CC was investigated as an anode for an MFC operated with real wastewater. Modifying the carbon cloth with a thin layer of iron significantly enhanced the performance of the MFC. This is because the power and current densities increased twice and three times, respectively, compared to those of using bare carbon cloth CC. The improved performance of the Fe-CC can be credited to the role of iron in improving the electron transfer between the microorganisms and the anode surface, as well as the increased surface area of the anode. This is evident from both the roughness and nanosheet structure of the Fe-CC electrode.

Author Contributions: Conceptualization, E.T.S. and M.A.A. (Muhammad Ali Abdelkareem); methodology, E.T.S., M.A.A. (Muhammad Ali Abdelkareem), S.T.B.T., and G.H.M.A.; validation, H.A., A.G.O., K.E.; formal analysis, H.A., A.G.O., K.E., and M.A.A. (Muhammad Ali Abdelkareem); writing—original draft preparation, E.T.S., H.A., K.E., A.G.O., M.A.A. (Muhammad Ali Abdelkareem); writing—review and editing, E.T.S., H.A., K.E., A.G.O., M.A.A. (Maryam Adel Almakrani); supervision, H.A., and A.G.O. All authors have read and agreed to the published version of the manuscript.

Funding: This research received no external funding.

Acknowledgments: This work was funded through the University of Sharjah, project No. 19020406129.

Conflicts of Interest: The authors declare no conflict of interest.

References

1. Wilberforce, T.; Baroutaji, A.; Soudan, B.; Al-Alami, A.H.; Olabi, A.G. Outlook of carbon capture technology and challenges. *Sci. Total Environ.* **2019**, *657*, 56–72. [CrossRef]
2. Elsaid, K.; Sayed, E.T.; Abdelkareem, M.A.; Baroutaji, A.; Olabi, A.G. Environmental impact of desalination processes: Mitigation and control strategies. *Sci. Total Environ.* **2020**, *740*, 140125. [CrossRef]
3. Elsaid, K.; Sayed, E.T.; Abdelkareem, M.A.; Mahmoud, M.S.; Ramadan, M.; Olabi, A.G. Environmental impact of emerging desalination technologies: A preliminary evaluation. *J. Environ. Chem. Eng.* **2020**, *8*, 104099. [CrossRef]
4. Elsaid, K.; Taha Sayed, E.; Yousef, B.A.A.; Kamal Hussien Rabaia, M.; Ali Abdelkareem, M.; Olabi, A.G. Recent progress on the utilization of waste heat for desalination: A review. *Energy Convers. Manag.* **2020**, *221*, 113105. [CrossRef]
5. Nassef, A.M.; Fathy, A.; Sayed, E.T.; Abdelkareem, M.A.; Rezk, H.; Tanveer, W.H.; Olabi, A.G. Maximizing SOFC performance through optimal parameters identification by modern optimization algorithms. *Renew. Energy* **2019**, *138*, 458–464. [CrossRef]
6. Abdelkareem, M.A.; El Haj Assad, M.; Sayed, E.T.; Soudan, B. Recent progress in the use of renewable energy sources to power water desalination plants. *Desalination* **2018**, *435*, 97–113. [CrossRef]
7. Abdelkareem, M.A.; Tanveer, W.H.; Sayed, E.T.; Assad, M.E.H.; Allagui, A.; Cha, S.W. On the technical challenges affecting the performance of direct internal reforming biogas solid oxide fuel cells. *Renew. Sustain. Energy Rev.* **2019**, *101*, 361–375. [CrossRef]

8. Inayat, A.; Nassef, A.M.; Rezk, H.; Sayed, E.T.; Abdelkareem, M.A.; Olabi, A.G. Fuzzy modeling and parameters optimization for the enhancement of biodiesel production from waste frying oil over montmorillonite clay K-30. *Sci. Total Environ.* **2019**, *666*, 821–827. [CrossRef] [PubMed]
9. Olabi, A.G.; Mahmoud, M.; Soudan, B.; Wilberforce, T.; Ramadan, M. Geothermal based hybrid energy systems, toward eco-friendly energy approaches. *Renew. Energy* **2020**, *147*, 2003–2012. [CrossRef]
10. Mahmoud, M.; Ramadan, M.; Olabi, A.-G.; Pullen, K.; Naher, S. A review of mechanical energy storage systems combined with wind and solar applications. *Energy Convers. Manag.* **2020**, *210*, 112670. [CrossRef]
11. Marx, H.; Forin, S.; Finkbeiner, M. Organizational Life Cycle Assessment of a Service Providing SME for Renewable Energy Projects (PV and Wind) in the United Kingdom. *Sustainability* **2020**, *12*, 4475. [CrossRef]
12. Rezk, H.; Alsaman, A.S.; Al-Dhaifallah, M.; Askalany, A.A.; Abdelkareem, M.A.; Nassef, A.M. Identifying optimal operating conditions of solar-driven silica gel based adsorption desalination cooling system via modern optimization. *Sol. Energy* **2019**, *181*, 475–489. [CrossRef]
13. Gomaa, M.R.; Mustafa, R.J.; Rezk, H. An experimental implementation and testing of a concentrated hybrid photovoltaic/thermal system with monocrystalline solar cells using linear Fresnel reflected mirrors. *Int. J. Energy Res.* **2019**, *43*, 8660–8673. [CrossRef]
14. Rezk, H.; Al-Oran, M.; Gomaa, M.R.; Tolba, M.A.; Fathy, A.; Abdelkareem, M.A.; Olabi, A.G.; El-Sayed, A.H.M. A novel statistical performance evaluation of most modern optimization-based global MPPT techniques for partially shaded PV system. *Renew. Sustain. Energy Rev.* **2019**, *115*, 109372. [CrossRef]
15. Fathy, A.; Elaziz, M.A.; Sayed, E.T.; Olabi, A.G.; Rezk, H. Optimal parameter identification of triple-junction photovoltaic panel based on enhanced moth search algorithm. *Energy* **2019**, *188*, 116025. [CrossRef]
16. Rezk, H.; Sayed, E.T.; Al-Dhaifallah, M.; Obaid, M.; El-Sayed, A.H.M.; Abdelkareem, M.A.; Olabi, A.G. Fuel cell as an effective energy storage in reverse osmosis desalination plant powered by photovoltaic system. *Energy* **2019**, *175*, 423–433. [CrossRef]
17. Wilberforce, T.; El Hassan, Z.; Durrant, A.; Thompson, J.; Soudan, B.; Olabi, A.G. Overview of ocean power technology. *Energy* **2019**, *175*, 165–181. [CrossRef]
18. Abdelkareem, M.A.; Sayed, E.T.; Mohamed, H.O.; Obaid, M.; Rezk, H.; Chae, K.-J. Nonprecious anodic catalysts for low-molecular-hydrocarbon fuel cells: Theoretical consideration and current progress. *Prog. Energy Combust. Sci.* **2020**, *77*, 100805. [CrossRef]
19. Abdelkareem, M.A.; Allagui, A.; Sayed, E.T.; El Haj Assad, M.; Said, Z.; Elsaid, K. Comparative analysis of liquid versus vapor-feed passive direct methanol fuel cells. *Renew. Energy* **2019**, *131*, 563–584. [CrossRef]
20. Abdelkareem, M.A.; Sayed, E.T.; Nakagawa, N. Significance of diffusion layers on the performance of liquid and vapor feed passive direct methanol fuel cells. *Energy* **2020**, *209*, 118492. [CrossRef]
21. Rezk, H.; Nassef, A.M.; Abdelkareem, M.A.; Alami, A.H.; Fathy, A. Comparison among various energy management strategies for reducing hydrogen consumption in a hybrid fuel cell/supercapacitor/battery system. *Int. J. Hydrog. Energy* **2019**. [CrossRef]
22. Abdelkareem, M.A.; Sayed, E.T.; Alawadhi, H.; Alami, A.H. Synthesis and testing of cobalt leaf-like nanomaterials as an active catalyst for ethanol oxidation. *Int. J. Hydrog. Energy* **2020**, *45*, 17311–17319. [CrossRef]
23. Sayed, E.T.; Nakagawa, N. Critical issues in the performance of yeast based microbial fuel cell. *J. Chem. Technol. Biotechnol.* **2018**, *93*, 1588–1594. [CrossRef]
24. Mohamed, H.O.; Obaid, M.; Sayed, E.T.; Abdelkareem, M.A.; Park, M.; Liu, Y.; Kim, H.-Y.; Barakat, N.A.M. Graphite Sheets as High-Performance Low-Cost Anodes for Microbial Fuel Cells Using Real Food Wastewater. *Chem. Eng. Technol.* **2017**, *40*, 2243–2250. [CrossRef]
25. Mohamed, H.O.; Abdelkareem, M.A.; Obaid, M.; Chae, S.-H.; Park, M.; Kim, H.Y.; Barakat, N.A.M. Cobalt oxides-sheathed cobalt nano flakes to improve surface properties of carbonaceous electrodes utilized in microbial fuel cells. *Chem. Eng. J.* **2017**, *326*, 497–506. [CrossRef]
26. Bolton, C.R.; Randall, D.G. Development of an integrated wetland microbial fuel cell and sand filtration system for greywater treatment. *J. Environ. Chem. Eng.* **2019**, *7*, 103249. [CrossRef]
27. Ali Ansari, S.; Mansoob Khan, M.; Omaish Ansari, M.; Hwan Cho, M. Improved electrode performance in microbial fuel cells and the enhanced visible light-induced photoelectrochemical behaviour of PtOx@M-TiO2 nanocomposites. *Ceram. Int.* **2015**, *41*, 9131–9139. [CrossRef]
28. De Sá, J.S.; Mezzomo, H.; Fraga, M.F.; Ogrodowski, C.S.; Santana, F.B. Anode air exposure during microbial fuel cell operation inoculated with marine sediment. *J. Environ. Chem. Eng.* **2017**, *5*, 1821–1827. [CrossRef]

29. Fazli, N.; Mutamim, N.S.A.; Jafri, N.M.A.; Ramli, N.A.M. Microbial Fuel Cell (MFC) in treating spent caustic wastewater: Varies in Hydraulic Retention Time (HRT) and Mixed Liquor Suspended Solid (MLSS). *J. Environ. Chem. Eng.* **2018**, *6*, 4339–4346. [CrossRef]
30. Sayed, E.T.; Shehata, N.; Abdelkareem, M.A.; Atieh, M.A. Recent progress in environmentally friendly bio-electrochemical devices for simultaneous water desalination and wastewater treatment. *Sci. Total Environ.* **2020**, 141046. [CrossRef]
31. Olabi, A.G.; Wilberforce, T.; Sayed, E.T.; Elsaid, K.; Rezk, H.; Abdelkareem, M.A. Recent progress of graphene based nanomaterials in bioelectrochemical systems. *Sci. Total Environ.* **2020**, 141225. [CrossRef]
32. Mohan, S.V.; Pandey, A.; Varjani, S. *Biomass, Biofuels, Biochemicals: Microbial Electrochemical Technology: Sustainable Platform for Fuels, Chemicals and Remediation*; Elsevier: Amsterdam, The Netherlands, 2018.
33. Pandit, S.; Savla, N.; Jung, S.P. Recent advancements in scaling up microbial fuel cells. In *Integrated Microbial Fuel Cells for Wastewater Treatment*; Abbassi, R., Yadav, A.K., Khan, F., Garaniya, V., Eds.; Butterworth-Heinemann: Waltham, MA, USA, 2020.
34. Abdallah, M.; Feroz, S.; Alani, S.; Sayed, E.T.; Shanableh, A. Continuous and scalable applications of microbial fuel cells: A critical review. *Rev. Environ. Sci. Bio/Technol.* **2019**, *18*, 543–578. [CrossRef]
35. Fan, L.; Xue, S. Overview on electricigens for microbial fuel cell. *Open Biotechnol. J.* **2016**, *10*, 398–406. [CrossRef]
36. Abdelkareem, M.A.; Masdar, M.S.; Tsujiguchi, T.; Nakagawa, N.; Sayed, E.T.; Barakat, N.A.M. Elimination of toxic products formation in vapor-feed passive DMFC operated by absolute methanol using air cathode filter. *Chem. Eng. J.* **2014**, *240*, 38–44. [CrossRef]
37. Kasem, E.T.; Tsujiguchi, T.; Nakagawa, N. Effect of Metal Modification to Carbon Paper Anodes on the Performance of Yeast-Based Microbial Fuel Cells Part I: In the Case without Exogenous Mediator. *Key Eng. Mater.* **2013**, *534*, 76–81. [CrossRef]
38. Sayed, E.T.; Barakat, N.A.; Abdelkareem, M.A.; Fouad, H.; Nakagawa, N. Yeast extract as an effective and safe mediator for the baker's-yeast-based microbial fuel cell. *Ind. Eng. Chem. Res.* **2015**, *54*, 3116–3122. [CrossRef]
39. Christwardana, M.; Frattini, D.; Accardo, G.; Yoon, S.P.; Kwon, Y. Effects of methylene blue and methyl red mediators on performance of yeast based microbial fuel cells adopting polyethylenimine coated carbon felt as anode. *J. Power Sources* **2018**, *396*, 1–11. [CrossRef]
40. Schaetzle, O.; Barrière, F.; Baronian, K. Bacteria and yeasts as catalysts in microbial fuel cells: Electron transfer from micro-organisms to electrodes for green electricity. *Energy Environ. Sci.* **2008**, *1*, 607–620. [CrossRef]
41. Yuan, Y.; Kim, S.-H. Improved performance of a microbial fuel cell with polypyrrole/carbon black composite coated carbon paper anodes. *Bull. Korean Chem. Soc.* **2008**, *29*, 1344–1348.
42. Zhao, F.; Rahunen, N.; Varcoe, J.R.; Chandra, A.; Avignone-Rossa, C.; Thumser, A.E.; Slade, R.C. Activated carbon cloth as anode for sulfate removal in a microbial fuel cell. *Environ. Sci. Technol.* **2008**, *42*, 4971–4976. [CrossRef]
43. Hidalgo, D.; Tommasi, T.; Bocchini, S.; Chiolerio, A.; Chiodoni, A.; Mazzarino, I.; Ruggeri, B. Surface modification of commercial carbon felt used as anode for microbial fuel cells. *Energy* **2016**, *99*, 193–201. [CrossRef]
44. Lanas, V.; Ahn, Y.; Logan, B.E. Effects of carbon brush anode size and loading on microbial fuel cell performance in batch and continuous mode. *J. Power Sources* **2014**, *247*, 228–234. [CrossRef]
45. Jung, S.P.; Pandit, S. Chapter Important Factors Influencing Microbial Fuel Cell Performance. In *Microbial Electrochemical Technology*; Mohan, S.V., Varjani, S., Pandey, A., Eds.; Elsevier: Amsterdam, The Netherlands, 2019.
46. Sayed, E.T.; Abdelkareem, M.A. Yeast as a biocatalyst in microbial fuel cell. *Old Yeasts-New Quest. InTech* **2017**, 41–65. [CrossRef]
47. Nam, T.; Son, S.; Koo, B.; Hoa Tran, H.V.; Kim, J.R.; Choi, Y.; Jung, S.P. Comparative evaluation of performance and electrochemistry of microbial fuel cells with different anode structures and materials. *Int. J. Hydrog. Energy* **2017**, *42*, 27677–27684. [CrossRef]
48. Jung, S.; Mench, M.M.; Regan, J.M. Impedance Characteristics and Polarization Behavior of a Microbial Fuel Cell in Response to Short-Term Changes in Medium pH. *Environ. Sci. Technol.* **2011**, *45*, 9069–9074. [CrossRef]

49. Kang, H.; Jeong, J.; Gupta, P.L.; Jung, S.P. Effects of brush-anode configurations on performance and electrochemistry of microbial fuel cells. *Int. J. Hydrog. Energy* **2017**, *42*, 27693–27700. [CrossRef]
50. Jung, S.P.; Kim, E.; Koo, B. Effects of wire-type and mesh-type anode current collectors on performance and electrochemistry of microbial fuel cells. *Chemosphere* **2018**, *209*, 542–550. [CrossRef]
51. Li, S.; Cheng, C.; Thomas, A. Carbon-based microbial-fuel-cell electrodes: From conductive supports to active catalysts. *Adv. Mater.* **2017**, *29*, 1602547. [CrossRef]
52. Khare, P.; Ramkumar, J.; Verma, N. Carbon nanofiber-skinned three dimensional Ni/carbon micropillars: High performance electrodes of a microbial fuel cell. *Electrochim. Acta* **2016**, *219*, 88–98. [CrossRef]
53. Zeng, L.; Zhao, S.; Wang, Y.; Li, H.; Li, W. Ni/β-Mo2C as noble-metal-free anodic electrocatalyst of microbial fuel cell based on Klebsiella pneumoniae. *Int. J. Hydrog. Energy* **2012**, *37*, 4590–4596. [CrossRef]
54. Zeng, L.-Z.; Zhao, S.-F.; Li, W.-S. Ni_3Mo_3C as anode catalyst for high-performance microbial fuel cells. *Appl. Biochem. Biotechnol.* **2015**, *175*, 2637–2646. [CrossRef] [PubMed]
55. Hindatu, Y.; Annuar, M.; Gumel, A. Mini-review: Anode modification for improved performance of microbial fuel cell. *Renew. Sustain. Energy Rev.* **2017**, *73*, 236–248. [CrossRef]
56. Wei, J.; Liang, P.; Huang, X. Recent progress in electrodes for microbial fuel cells. *Bioresour. Technol.* **2011**, *102*, 9335–9344. [CrossRef] [PubMed]
57. Liu, X.; Du, X.; Wang, X.; Li, N.; Xu, P.; Ding, Y. Improved microbial fuel cell performance by encapsulating microbial cells with a nickel-coated sponge. *Biosens. Bioelectron.* **2013**, *41*, 848–851. [CrossRef]
58. Xie, W.; Guo, Z.; Gao, F.; Gao, Q.; Wang, D.; Liaw, B.-S.; Cai, Q.; Sun, X.; Wang, X.; Zhao, L. Shape-, size- and structure-controlled synthesis and biocompatibility of iron oxide nanoparticles for magnetic theranostics. *Theranostics* **2018**, *8*, 3284–3307. [CrossRef]
59. Wang, L.; Wang, Z.; Li, X.; Zhang, Y.; Yin, M.; Li, J.; Song, H.; Shi, J.; Ling, D.; Wang, L. Deciphering active biocompatibility of iron oxide nanoparticles from their intrinsic antagonism. *Nano Res.* **2018**, *11*, 2746–2755. [CrossRef]
60. Janko, C.; Zaloga, J.; Pöttler, M.; Dürr, S.; Eberbeck, D.; Tietze, R.; Lyer, S.; Alexiou, C. Strategies to optimize the biocompatibility of iron oxide nanoparticles–"SPIONs safe by design". *J. Magn. Magn. Mater.* **2017**, *431*, 281–284. [CrossRef]
61. Lowy, D.A.; Tender, L.M.; Zeikus, J.G.; Park, D.H.; Lovley, D.R. Harvesting energy from the marine sediment–water interface II: Kinetic activity of anode materials. *Biosens. Bioelectron.* **2006**, *21*, 2058–2063. [CrossRef]
62. Glass, D.E.; Galvan, V.; Prakash, G.K.S. The Effect of Annealing Temperature on Nickel on Reduced Graphene Oxide Catalysts on Urea Electrooxidation. *Electrochim. Acta* **2017**, *253*, 489–497. [CrossRef]